Biosensors and Bioelectronics 126 (2019) 529–534

Contents lists available at ScienceDirect

Biosensors and Bioelectronics

journal homepage: www.elsevier.com/locate/bios

Copper ion-assisted gold nanoparticle aggregates for electrochemical signal amplification of lipopolysaccharide sensing

Nan Wang[a], Hongxiu Dai[a,c], Lintao Sai[b], Houyi Ma[a,*], Meng Lin[a,*]

[a] Key Laboratory for Colloid and Interface Chemistry of State Education Ministry, School of Chemistry and Chemical Engineering, Shandong University, Jinan 250100, China

[b] Department of Infectious Diseases, Qilu Hospital of Shandong University, Jinan 250012, China

[c] Department of Chemistry, Liaocheng University, Liaocheng 252059, China

ARTICLE INFO

Keywords:
Lipopolysaccharide
Aptasensor
Gold nanoparticles
Copper ions
Signal amplification

ABSTRACT

A signal amplification electrochemical aptasensor for ultrasensitive detection of lipopolysaccharide (LPS) was fabricated. The sensor was constructed with a probe of LPS aptamer and a copper ions-mediated gold nanoparticles aggregate (Cu/Au NA) as a signal amplification material. The Cu/Au NAs comprising copper ions (Cu^{2+}) and L-cysteine modified AuNPs were fabricated by a self-assembly process. For functionalization of the electrode, the carboxylic group of a mercaptoacetic acid self-assembly layer was covalently coupled with the amine group of the aptamer. The aptamer with high specificity and affinity can effectively gather the dissociative LPS firstly, and the Cu/Au NAs were captured by anionic groups of the carbohydrate portions from LPS molecules based on the specific interactions. With the employment of the sandwich-type biosensor, the strategy can significantly amplify the electrochemical signal for determination of trace amount of LPS. The sensing performance of the electrochemical sensor was investigated by differential pulse voltammetry (DPV) and the stripping peak currents of Cu re-oxidized to Cu^{2+} was used to monitor the level of LPS. The electrochemical aptasensor exhibited excellent sensitivity toward LPS with a detection limit of 0.033 pg/mL (S/N = 3). The biosensor also exhibited a high specificity toward LPS in the presence of other common interfering substances and was easily regenerated. Furthermore, the fabricated biosensor showed a good practical application for LPS determination in human serum samples.

1. Introduction

Lipopolysaccharide (LPS), known as endotoxin, is one of the components of the outer membrane of gram-negative bacteria. Trace amounts of endotoxin can cause high body temperature and a series of harmful symptoms, such as asthma, septic shock, diarrhea and so on (Bai et al., 2014). So, rapid and sensitive determination of LPS is critical to the safety and security in foodstuff and medical supplies. In recent years, the LPS sensors based on numbers of LPS-binding proteins, peptides and artificial affinity recognizing molecules are reported (Su et al., 2012; Jones and Jiang, 2005; Limbut et al., 2007). Chang et al. uncovered an electrochemical impedance spectroscopic method to detect LPS by using polymyxin B immobilized on gold electrodes (Ding et al., 2007), and a peptide-modified electrode utilized to detect endotoxin was reported by Miao and co-workers (Liu et al., 2017). All of these endotoxin detection methods rely on above reagents are well-proven and widely accepted. But the previous approaches could be limited, because of the common sandwich-type sensors cannot be structured due to the single combining site between LPS and recognizing molecules (Bai et al., 2014).

To achieve a low detection level of LPS, signal multiplication technology is required to design (Shen et al., 2015). For instance, Niwa et al. reported a ferrocenylboronic acid-based signal amplification method using an enzyme-modified electrode for the detection of LPS in a low concentration (Kato et al., 2007). However, the approach suffered from inactivation of enzyme, contaminated and complicated preparation. Owing to the essential advantages such as relative ease of synthesis, high stability and conductivity, good biocompatibility and high affinity of binding to amine/thiol-containing molecules, gold nanoparticles (AuNPs) have been used in the field of LPS sensors (Wang et al., 2014, 2016; Lin, 2015). For example, Wang et al. reported a colorimetric method for the detection of endotoxin based on the electrostatic interaction between LPS molecules and cysteamine modified AuNPs (Sun et al., 2012). Yuan and co-workers utilized AuNPs modified

* Corresponding authors.
E-mail addresses: hyma@sdu.edu.cn (H. Ma), mlin@sdu.edu.cn (M. Lin).

https://doi.org/10.1016/j.bios.2018.11.021
Received 18 September 2018; Received in revised form 14 November 2018; Accepted 14 November 2018
Available online 16 November 2018
0956-5663/

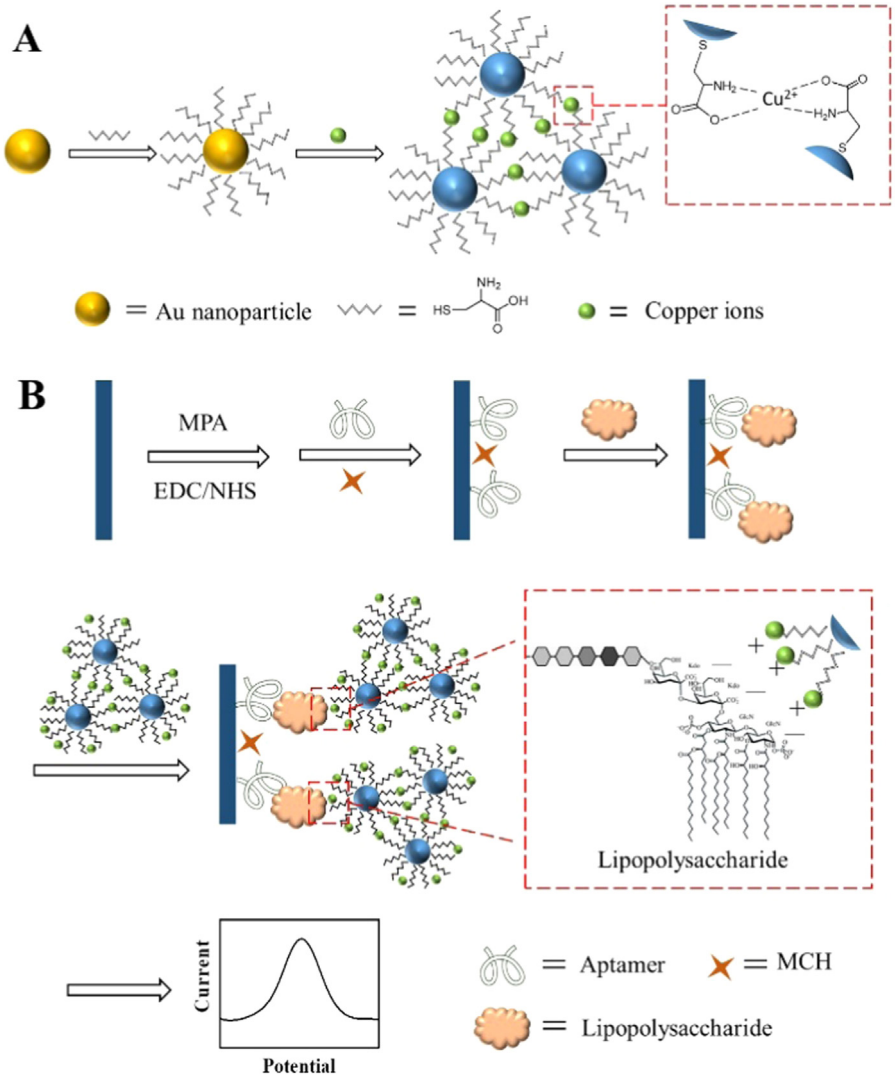

Scheme 1. (A) Preparation of copper ions-mediated gold nanoparticles aggregate. (B) Fabrication of a sandwich-type electrochemical LPS aptasensor.

Ce-based metal-organic frameworks for LPS sensing based on DNAzyme-assisted recycle process (Shen et al., 2016). Electrochemical aptasensors based AuNPs modified electrodes for LPS detection was also reported (Posha et al., 2018; Su et al., 2013). In the use of Au NPs for LPS analysis, a little attention has been paid to metal ions-mediated AuNPs aggregate based on signal amplification strategy for electrochemical LPS sensing.

Predicted from the intrinsic structure, the highly anionic LPS molecule (lipid A, core oligosaccharide, and O-specific antigen) can combine with divalent ions (such as Cu^{2+}, Ni^{2+} and Zn^{2+}) through specific interactions of anionic groups in the carbohydrate portions (Ho et al., 1998). Therefore, we developed an electrochemical LPS aptasensor using a copper ions-mediated gold nanoparticles aggregate (Cu/Au NA) for the signal enlargement platform (Scheme 1). The AuNPs acted as a carrier for copper ions (Cu^{2+}) resulting from a function of L-cysteine bridge modification. After the aptamer specific combined with LPS, Cu^{2+} from Cu/Au NA could easily bind to the O-side chain of LPS molecule and the Cu/Au NA containing huge amounts of Cu^{2+} can enhance the analytical signal through sandwich-type recognition reaction. The Cu^{2+} in the aptamer-LPS-Cu/Au NA matrix could be electrochemically detected directly, by measuring the re-oxidation current of copper, the differential pulse stripping voltammetric response was proportional to the amount of LPS bound to the aptamer, which gave the quantitative criteria for the detection of LPS. The strategy illustrated an excellent signal amplification platform, and the fabricated LPS sensor presented a linear range from 0.05 pg/mL to 10 pg/mL with a detection limit of 0.033 pg/mL. Furthermore, the biosensor was successfully applied to ultrasensitive determination of LPS in human serum samples.

2. Experimental section

2.1. Materials and reagents

Hydrogen tetrachloroaurate(III) trihydrate ($HAuCl_4{\cdot}3H_2O$), sodium citrates, potassium ferricyanide ($K_3[Fe(CN)_6]$) and potassium ferrocyanide trihydrate ($K_4[Fe(CN)_6]{\cdot}3H_2O$) were obtained from Sinopharm Chemical Reagent Co., Ltd. L-cysteine hydrochloride, copper ions standard stock solutions, mercaptoacetic acid (MPA), mercaptoethanol (MCH), N-(3-dimethylaminopropyl)-N′-ethylcarbodiimide hydrochloride (EDC), N-hydroxy-succinimide (NHS) and morpholinoethanesulfonic acid (MES) were purchased from Aldrich (Shanghai, China). The aptamer, NH_2–5′-CTTCTG CCC GCC TCC TTC C- TAG CCG GAT CGC GCT GGC CAG ATG ATA TAA AGG GTC AGC CCC CCA GGA GAC GAG ATA GGC GGA CAC T-3′ was purchased from Sangon Biotech Co., Ltd. (Shanghai, China). LPS from *Escherichia coli 055:B5* was purchased from Sigma and stored at −4 °C. Gold disk electrode (d = 2.0 mm) was purchased from Tianjin Ada Hengsheng Technology Co., Ltd. Ultrapure

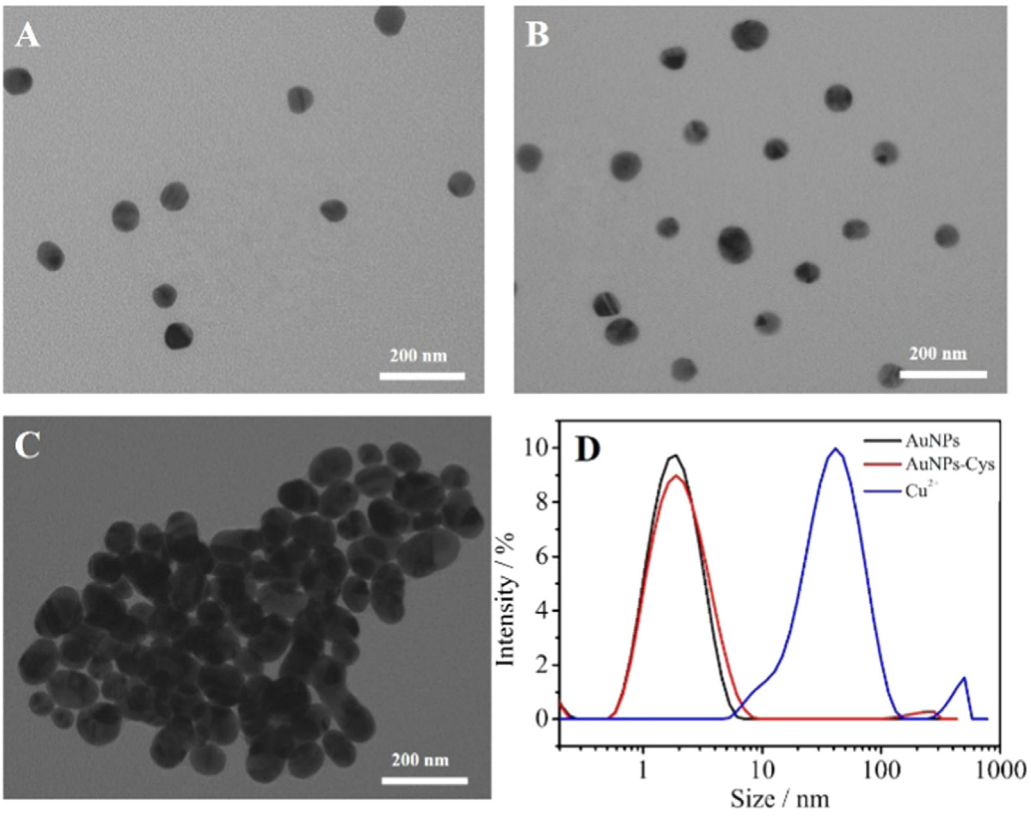

Fig. 1. TEM images of AuNPs (A), L-cysteine modified AuNPs (B) and the Cu/Au NAs (C). The corresponding particle size distribution of the original AuNPs (black line), L-cysteine modified AuNPs (red line) and the Cu/Au NAs (blue line). (For interpretation of the references to color in this figure legend, the reader is referred to the web version of this article).

water (≥ 18 MΩ cm) was used throughout the experiments. Limulus Amebocyte Lysate (LAL) was obtained from Xiamen Limulus Reagent Biotechnology Co., Ltd. All other chemicals were used of analytical reagent grade or better without further purification

2.2. Apparatus

Morphology of nanomaterials were obtained by transmission electron microscopy (TEM, JEM-1011) with an acceleration voltage of 100 kV. Absorption spectra were recorded by UV–vis spectroscopy (Thermo Evolution 220) at room temperature. Attenuated total reflection infrared (ATR-IR) spectra were obtained by infrared spectrophotometry (Nicolet IS5, Thermo Fisher Scientific) and the resolution of 2 cm^{-1} with a total of 16 scans. X-ray photoelectron spectroscopy (XPS) was performed on VG ESCALAB 220i-XL instrument with a monochromatic Al Kα X-ray source. The size distribution was measured by a Zetasizer Nano-ZS instrument (ZEN3600, Malvern Instruments, Worcestershire, UK). Differential pulse voltammetry (DPV) was performed on a CHI750E electrochemical workstation (Shanghai Chen hua Instruments, China) with a three-electrode cell. Electrochemical impedance spectroscopy (EIS) and cyclic voltammetry (CV) were evaluated using an electrochemical system (HZ-7000, Hokuto Denko). All electrochemical analysis was programmed with respect to a saturated calomel electrode (SCE, with a saturated KCl solution) as a reference electrode, and a platinum plate as a counter electrode.

2.3. Preparation of copper ions-mediated gold nanoparticles aggregate

AuNPs were prepared according to a previous report with a mean diameter of 17 nm (Frens, 1973). Subsequently, 5.0 mL AuNPs solution (2.5×10^{-4} M) was mixed with a L-cysteine solution (0.40 μM) and gently stirred for 4 h. The L-cysteine functionalized AuNPs were centrifugated at 10000 rpm for 15 min to remove the dissociative L-cysteine molecules, and redispersed by 0.1 mM pH = 5.5 phosphate buffer solution. After addition of various concentrations of Cu^{2+}, the aggregation of the AuNPs was happened along with an immediate color change from red to bluish violet and the copper ions-mediated gold nanoparticles aggregate (Cu/Au NA) was formed (Yang et al., 2007).

2.4. Fabrication of LPS aptasensor

Gold disk electrode (active diameter 2 mm) was polished to a mirror surface by using 1.0, 0.3, and 0.05 μm alumina slurry, and successive sonication in 1:1 nitric acid, ethanol and deionized water, respectively. In order to obtain aptamer modified gold electrode, the gold electrode immersed into a 20 mM MPA solution for 12 h at first, and then the pretreated electrode was putted into a phosphate buffer solution (10 mM, pH = 7.4) containing 0.05 M EDC and 0.02 M NHS for activating the carboxyl-terminated group of MPA. After carefully washed with distilled water, 40 μL of 0.2 μM aptamer in phosphate buffer solution (10 mM, pH 7.4) was dropped onto the electrode surface, and the amino-functioned aptamer could be anchored through amidation reaction. Prior to incubation process, the aptamer modified electrode was thoroughly rinsed and immersed into 1.0 mM MCH solution for 1.0 h in order to block the remaining bare region. Then, the modified electrode incubated with 10 μL of different concentrations of LPS at 37 °C for 60 min.

2.5. Electrochemical analysis of LPS

As a signal amplification probe, a constant concentration of Cu/Au NA was captured on the surface of biosensor through the specific recognition between the Cu^{2+} and LPS for forming a typical sandwiched sensor. The electrochemical measurement was performed in 10 mM phosphate buffer solution (pH = 7.4). Before DPV measurements, a prereduced step with an applied potential of −0.4 V for direct reduction of Cu^{2+} to Cu about 240 s. Then electrochemical response of the labeled Cu^{2+} came from the Cu/Au NA was recorded by differential pulse voltammetry (DPV) from −0.4 to + 0.4 V at an amplitude of 20 mV, a pulse width of 0.05 s, a pulse period of 0.2 s and quiet time of 2 s. The

stripping response of Cu^{2+} was supported in quantitative analysis of LPS. The comparative DPV response of the LPS sensor labeled by free Cu^{2+} was further studied.

3. Results and discussion

3.1. Morphological characterization of the Cu/Au NAs

The optimum conditions for the preparation of Cu/Au NA was described in Supporting information and Fig. S1. Existence forms of AuNPs with the original (Fig. 1A) and aggregated were characterized by TEM. Compared with the L-cysteine functionalized AuNPs (Fig. 1B), the addition of Cu^{2+} gives rise to significant aggregation of AuNPs (Fig. 1C). The results confirm that the Cu^{2+} can serve as a bridge between the L-cysteine functionalized AuNPs for the formation of Cu/Au NAs. Size distributions of the AuNPs before and after modification with L-cysteine and copper ions are plotted in Fig. 1D. After the assembly reaction, the size of the functionalized AuNPs remained almost similar to that of the AuNPs (from 17 nm to 20 nm) (Naka et al., 2003). After the interaction between L-cysteine-Au NPs and Cu^{2+}, the size distribution illustrates the formation of a large aggregate about 400 nm, which is in good agreement with the results from UV–vis spectra and TEM investigation.

3.2. Characterization of the aptasensor

Modification of MPA and aptamer to the gold electrode was characterized by ATR-IR. As Fig. S2 depicted, typical absorption peaks at 1712 cm^{-1} (C=O), 1288 cm^{-1} (C-O) indicating the anchoring of MPA molecule onto the surface of the electrode (Koneswaran and Narayanaswamy, 2009). The amide vibration at 1648 cm^{-1} and the bands in the region of 1600–1500 cm^{-1} attributed to the vibration of N-H, C=C and C=N of the base rings confirm that the aptamer successfully linked to MPA through amidation reaction (Wang et al., 2014a, 2014b; Dovbeshko et al., 2000). After the aptamer combined with LPS, two specific absorption peaks assigned to the ester double bond stretch and primarily ν(C=O) of LPS are displayed at 1745 cm^{-1} and 1682 cm^{-1}, respectively. The bands in the range of 1100–990 cm^{-1} correspond to the vibrations of unspecific sugar and phosphate groups from the O-polysaccharides (as an integral part of LPS) and the aptamer sequence (Dovbeshko et al., 2000; Brandenburg, 1993). In contrast, there is no any special absorption peak emerged after MCH blocking and Cu/Au NA labeled processes, because of the similar functional groups existed in the previous steps.

In order to prove the Cu/Au NA labelling process, the electrode was further confirmed by XPS analysis. S 2p peak attributes to MPA and MCH molecules, and P 2p peak derives from the aptamer and LPS (Fig. S3). High-resolution XPS spectrum of C 1s exhibits three peaks at 284.72, 286.30 and 287.66 eV (Fig. 2A) corresponded to C-C/C-H, C=O/C-O and C-OH bonds, respectively (Chandra et al., 2011). After LPS combination, as Fig. 2B observed, a new peak at 288.66 eV assigned to -O-C=O of lipid A (part of LPS) is appeared (Yang et al., 2011). In addition, the content of P element increased from 10.94% to 16.62% could further identify the participation of phosphoric acid groups from the core-lipid A region of the LPS (Patel et al., 2010). After the Cu/Au NAs labeled, the XPS spectrum of Cu element accounted for the presence of Cu/Au NAs emerges at 932.35 eV (Cu $2p_{3/2}$) and 952.9 eV (Cu $2p_{1/2}$) indicating the successful combination of Cu/Au NAs and LPS molecules (Fig. 3A) (Miao et al., 2013). The nitrogen can be fitted with three peaks (Fig. 3C) and a new peak contributed by nitrogen cationic at 407.1 eV could be assigned to N-Cu binding energy (Takayanagi et al., 2008), while the peaks with binding energies at 399.0 eV and 400.5 eV are ascribed to amine nitrogen (-NH) and amide nitrogen (-NH-CO) in Fig. 3B (Yun et al., 2011).

EIS and CV curves were also designed to characterize the stepwise fabrication processes of the aptasensor. In general, the diameter of the semicircle portion at higher frequencies represents the electron-transfer resistance, R_{et}, and the change of R_{et} is related to the different electrode modification processes (Su et al., 2012). As illustrated in Fig. S4A, typical Nyquist plots of the modified electrodes in 2 mM $Fe[(CN)_6]^{3-/4-}$ phosphate buffer solution (10 mM, pH 7.4) were recorded. The bare gold electrode has a relatively small semicircle (curve a) indicating a low resistance on the surface of the redox probe. After MPA modification, the increasing of semicircle diameter (curve b) implying the MPA was successfully self-assembled onto the gold electrode surface. When the aptamer was immobilized on the MPA/gold electrode, the semicircle continuing to rise (curve c). The probable reason is the electronegative groups of phosphate skeleton from the aptamer could prevent the negative $Fe[(CN)_6]^{3-/4-}$ ions arriving at the surface of the electrode and inhibit the electron transfer process of redox reaction (Zhu et al., 2013). After blocked with MCH, the electrochemical impedance increases gradually (curve d). Owing to the specifically affinity between LPS and aptamer, the semicircle diameter corresponded to the R_{et} increases significantly (curve e), with the negatively charged LPS adsorbed (Cho et al., 2012). Meanwhile, the value of R_{et} decreased with the addition of Cu/Au NA (curve f) demonstrates that the labeled Cu/Au NA can promote the electron-transfer between the modified electrode and electrolyte. Fig. S4B shows the CVs results of the electrode modification process in 2 mM $Fe[(CN)_6]^{3-/4-}$ KCl (0.1 M) aqueous solution with a scan rate of 50 mV s^{-1}. The value changes of approximately reversible redox peaks ascribed to the $Fe[(CN)_6]^{3-/4-}$ were quite consistent with the conclusion of the EIS studies, accounting for successful fabrication of the LPS aptasensor.

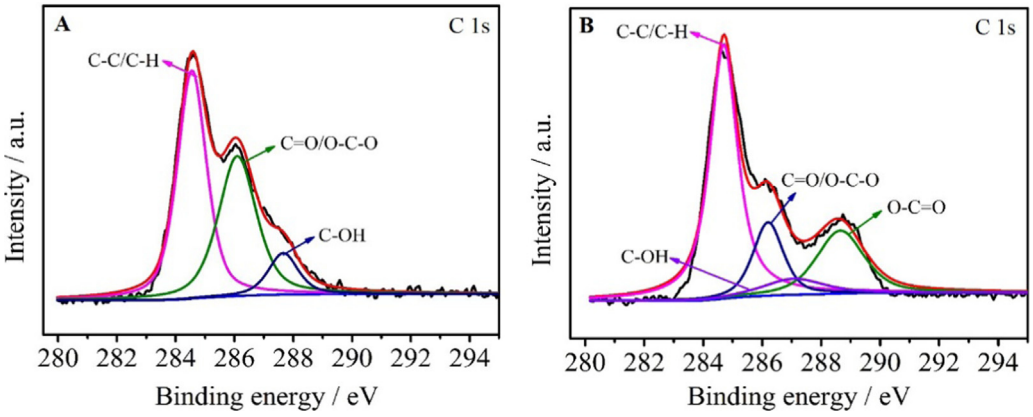

Fig. 2. High-resolution XPS spectra of C 1s region before (A) and after (B) combination with LPS.

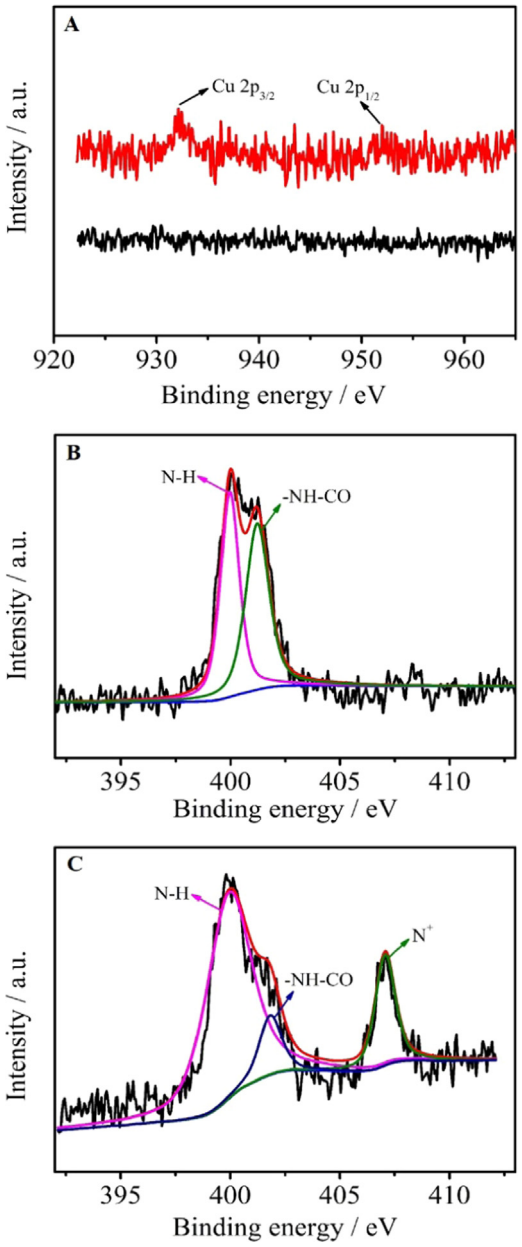

Fig. 3. High-resolution XPS spectra of Cu 2p and N 1s before (A black line and B) and after (A red line and C) the Cu/Au NA labeled to the biosensor, respectively. (For interpretation of the references to color in this figure legend, the reader is referred to the web version of this article).

3.3. Signal amplification properties of the Cu/Au NAs

In order to elucidate the effect of signal amplification, two kinds of probes (single Cu^{2+} and Cu/Au NAs) were utilized. Under the same concentration of LPS, a significant electrochemical response by the Cu/Au NAs (Fig. 4 curve c) observes than that of single Cu^{2+} labeled (Fig. 4 curve b). Cu^{2+} can be captured onto the surface of AuNPs by coordination with amino and carboxyl groups of L-cysteine to form gold nanoparticle aggregates, which could greatly enhance the amount of labeled Cu^{2+} incorporated with LPS. Therefore, even at a low concentration of LPS, the signal amplification strategy by the Cu/Au NAs labeled process can improve the sensitivity of the biosensor toward LPS.

3.4. Electrochemical performance of the biosensor

Under the optimal conditions (the effect of Cu^{2+} and incubation

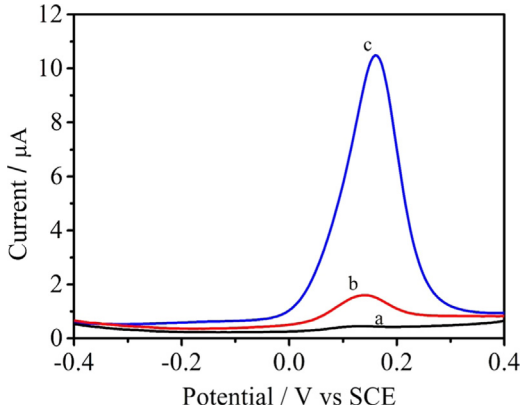

Fig. 4. DPV measurements toward 10 pg/mL LPS by the sandwich-type biosensor without (a), with Cu^{2+} (b) and 30 μL Cu/Au NA (c) labeled the aptamer electrodes.

time about the designed aptasensor are shown in Figs. S5 and S6), to evaluate the electrochemical performance of the fabricated aptasensor, the proposed aptamer-modified electrode was immersed into a 10 mM phosphate buffer solution (pH = 7.4) containing various concentrations of LPS. Then, dependent on the specific interactions, the LPS can be labeled with the Cu/Au NAs. By measuring the stripping current of Cu^{2+}, the electrochemical response is proportional to the amount of LPS bound to the aptamer, which is supported by the quantitative analysis of LPS (Fig. 5A). Fig. 5B shows two good linear relationships between the stripping peak currents and the LPS concentrations in the range from 0.05 pg/mL to 1.0 pg/mL with a correlation coefficient of R^2 = 0.987 and 1.0 to 10 pg/mL with a correlation coefficient of R^2

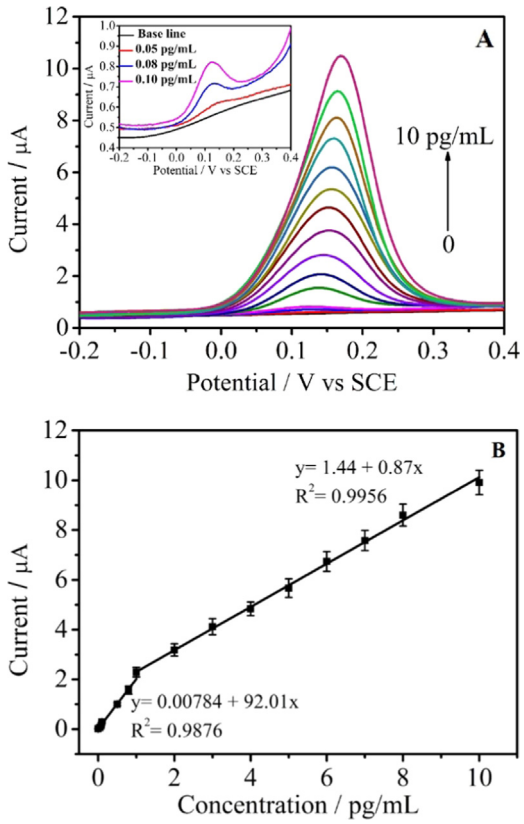

Fig. 5. (A) DPV responses of the fabricated biosensor to different concentrations of LPS using the Cu/Au NAs as signal label materials; (B) The corresponding calibration curves of the biosensor toward LPS at different concentrations (0.05–10 pg/mL).

= 0.996, respectively, and a detection limit of 0.033 pg/mL (S/N = 3) obtained. As Table S1 listed, compared with the previous literature, the proposed biosensor is found to have a good electrochemical sensing performance (detection range and the limit of detection) to LPS. The direct determination of the adsorbed Cu^{2+} on the electrode surface without adding extra and acid dissolution processes is beneficial for maintaining the activity of biological molecules. With the employment of sandwich-type sensor, the strategy can significantly amplify the electrochemical signal for highly sensitive and selective determination of trace amount of LPS.

3.5. Selectivity, reproducibility and stability

A series of contrast investigations on possible interferents, such as epinephrine (Epin), cholesterol (Chol), glucose (Glu) and uric acid (UA) were carried out, and the results are presented in Fig. S7. The developed aptasensor exhibits an unremarkable change of electrochemical response with and without the interfering substances during the measurements. Indistinguishable peak currents to the interferents, even the concentrations were 10 times than that of LPS, demonstrating the biosensor has a highly selectivity to the target analyte. In addition, the affinity of the LPS molecule toward divalent ions follows the order: $Cu^{2+} > Zn^{2+} > Ni^{2+}$, Co^{2+} (Tan et al., 2007). Prior to the re-oxidation current measurement by DPV method, a pre-reduced step for direct reduction of the pre-concentrated metal ions was implemented. By comparing the standard electrode potentials, only the Cu^{2+} can be reduced and tested under the experimental processes.

To assess the reproducibility of the proposed electrochemical sensor, three parallel prepared aptamer modified electrodes were incubated with the identical LPS concentration (5 pg/mL). After careful measurements and calculations, the relative standard deviation (RSD) of 4.29% is achieved. For the intra-assay precision, one aptamer modified electrode was used to detect the same concentration of LPS (5 pg/mL) for five repeated times, and the RSD is calculated as 1.36%. In addition, the peak current is retained 96% of the initial response after seven days storage at 4 °C. The results demonstrate that the LPS aptasensor has an acceptable reliability and stability.

3.6. Detection of LPS in human serum samples

Practical application in human serum samples with spiked a certain concentration of LPS was evaluated. Human blood samples were available from Qilu Hospital of Shandong University by volunteers. Prior to the testing, the samples were acquired by centrifugal separation, collected the supernatant, 50 fold-diluted serum samples and dispersed into 30 mL of phosphate buffer solution (10 mM, pH = 7.4). The level of LPS was monitored by our strategy and Limulus Amebocyte Lysate (LAL) assay. As Table S2 and Fig. S8 illustrated, the excellent performance of the sandwich-type electrochemical biosensor shows a good sensitivity to LPS, indicating that the sensor has a potential application for LPS detection in a complex environment.

4. Conclusions

In summary, we designed a sandwich-type electrochemical aptasensor for determination of endotoxin based on aptamer-functionalized gold nanoparticles modified electrodes and copper ions-assisted aggregates as an electrochemical signal amplification labels. The introduction of the Cu/Au NAs is not only conducive to simplify the analysis process, but also to amplify the electrochemical signal. Comparing with the labeled of single copper ions, the utilization of Cu/Au NAs greatly enhances the sensitivity of the LPS sensor. The electrochemical performance of the aptasensor, demonstrated for Cu^{2+} detection by differential pulse voltammetry, proved that the developed sensor is highly sensitive to indirectly detect LPS in the range from 0.05 pg to 10 pg/mL with easy operation, good stability and acceptable reproducibility. The sensor is applied to determine LPS in human serum samples suggesting that the proposed sensing configuration could be used for detection of non-bioelectroactive molecules in complex systems instead of the pricey antibody/antigen strategy. In addition, more efforts on assembling of the aptasensor devices are still required.

Acknowledgements

This work was supported by the Young Scholars Program of Shandong University, Shandong Provincial Natural Science Foundation, China (ZR2017QB004), the National Natural Science Foundation of China (21673130) and the Taishan Scholar Project of Shandong Province (ts201712011).

Appendix A. Supporting information

Supplementary data associated with this article can be found in the online version at doi:10.1016/j.bios.2018.11.021.

References

Bai, L.J., Chai, Y.Q., Pu, X., Yuan, R., 2014. Nanoscale 6, 2902–2908.
Brandenburg, K., 1993. Biophys. J. 64, 1215–1231.
Chandra, P.H., Noh, B., Won, M.S., Shim, Y.B., 2011. Biosens. Bioelectron. 26, 4442–4449.
Cho, M., Chun, L.M., Lin, M., Choe, W., Lee, Y., 2012. Sens. Actuators B 174, 490–494.
Ding, S.J., Chang, B.W., Wu, C.C., Chang, H.C., 2007. Electrochem. Commun. 9, 1206–1211.
Dovbeshko, G.I., Gridina, N.Y., Kruglova, E.B., Pashchuk, O.P., 2000. Talanta 53, 233–246.
Frens, G., 1973. Nat. Phys. Sci. 241, 20–22.
Ho, C.H., Limberis, L., Caldwell, K.D., Stewart, R.J., 1998. Langmuir 14, 3889–3894.
Jones, G., Jiang, H., 2005. Bioconjug. Chem. 16, 621–625.
Kato, D., Kurita, R., Sato, Y., Niwa, O., 2007. Biosens. Bioelectron. 22, 1527–1531.
Koneswaran, M., Narayanaswamy, R., 2009. Sens. Actuators B 139, 91–96.
Limbut, W., Hedström, M., Thavarungkul, P., Kanatharana, P., Mattiasson, B., 2007. Anal. Bioanal. Chem. 389, 517–525.
Lin, M., 2015. RSC Adv. 5, 9848–9851.
Liu, T., Meng, F., Cheng, W., Sun, H., Luo, Y., Miao, P., 2017. ACS Omega 2, 2469–2473.
Miao, L.J., Xin, J.W., Shen, Z.Y., Zhang, Y.J., Wang, H.Y., Wu, A.G., 2013. Sens. Actuators B 176, 906–912.
Naka, K., Itoh, H., Tampo, Y., Chujo, Y., 2003. Langmuir 19, 5546–5549.
Patel, M.K., Solanki, P.R., Kumar, A., Khare, S., Gupta, S., Malhotra, B.D., 2010. Biosens. Bioelectron. 25, 2586–2591.
Posha, B., Nambiar, S.R., Sandhyarani, N., 2018. Biosens. Bioelectron. 101, 199–205.
Shen, W.J., Zhuo, Y., Chai, Y.Q., Yuan, R., 2015. Anal. Chem. 87, 11345–11352.
Shen, W.J., Zhuo, Y., Chai, Y.Q., Yuan, R., 2016. Biosens. Bioelectron. 83, 287–292.
Su, W., Cho, M., Nam, J.D., Choe, W.S., Lee, Y., 2013. Electroanalysis 25, 380–386.
Su, W., Lin, M., Lee, H., Cho, M.S., Choe, W.S., Lee, Y., 2012. Biosens. Bioelectron. 32, 32–36.
Sun, J., Ge, J., Liu, W., Wang, X., Fan, Z., Zhao, W., Zhang, H., Wang, P., Lee, S.T., 2012. Nano Res. 5, 486–493.
Takayanagi, M., Imai, Y.K., Yokozawa, T., Tajima, K., 2008. J. Oleo Sci. 57, 233–242.
Tan, L., Lai, W.B., Lee, C.T., Kim, D.S., Choe, W.-S., 2007. J. Chromatogr. A 1141, 226–234.
Wang, N., Lin, M., Dai, H., Ma, H., 2016. Biosens. Bioelectron. 79, 320–326.
Wang, Y.H., Gao, D.Y., Zhang, P.F., Gong, P., Chen, C., Gao, G.H., Cai, L.T., 2014. Chem. Commun. 50, 811–813.
Wang, Y., Zhang, D., Liu, W., Zhang, X., Yu, S., Liu, T., Zhang, W., Zhu, W., Wang, J., 2014. Biosens. Bioelectron. 55, 242–248.
Yang, R., Liu, G.Q., Xu, X.H., Li, M., Zhang, J.C., Hao, X.M., 2011. Biomass Bioenergy. 35, 437–445.
Yang, W.R., Gooding, J.J., He, Z.C., Chen, G.N., 2007. J. Nanosci. Nanotechnol. 7, 712–716.
Yun, S.J., Im, H., Kim, J., 2011. Synth. Met. 61, 1361–1367.
Zhu, Y., Chandra, P., Shim, Y.B., 2013. Anal. Chem. 85, 1058–1064.